

A New Force Field of Formamide and the Effect of the Dielectric Constant on Miscibility

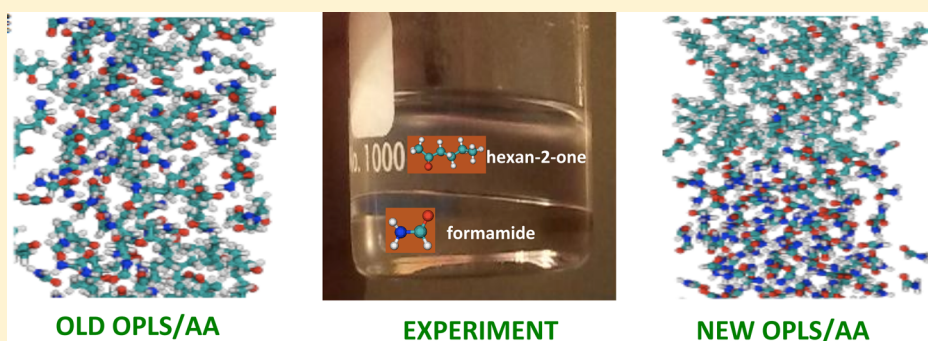
Alexander Pérez de la Luz,[†] G. Arlette Méndez-Maldonado,[†] Edgar Núñez-Rojas,[†] Fernando Bresme,^{‡,§} and José Alejandro^{*,†}

[†]Departamento de Química, Universidad Autónoma Metropolitana-Iztapalapa, Avenida San Rafael Atlixco 186, Col. Vicentina, 09340 México Distrito Federal, México

[‡]Department of Chemistry, Imperial College London, London SW7 2AZ, United Kingdom

[§]Department of Chemistry, Norwegian University of Science and Technology, NO-7491 Trondheim, Norway

S Supporting Information



ABSTRACT: Current force fields underestimate significantly the dielectric constant of formamide at standard conditions. We present a derivation of an accurate potential for formamide, with a functional form based on the OPLS/AA force field. Our procedure follows the approach introduced by Salas et al. (*J. Chem. Theory Comput.* **2015**, *11*, 683–693) that relies on *ab initio* calculations and molecular dynamics simulations. We consider several strategies to derive the atomic charges of formamide. We find that the inclusion of polarization effects in the quantum mechanical computations is essential to obtain reliable force fields. By varying the atomic charges and the Lennard-Jones parameters describing the dispersion interactions in the OPLS/AA force field, we derive an optimum set of parameters that provides accurate results for the dielectric constant, surface tension, and bulk density of liquid formamide in a wide range of thermodynamic states. We test the transferability of our parameters to investigate liquid/liquid mixtures. We have chosen as case study an equimolar mixture of formamide and hexan-2-one. This mixture involves two fluids with very different polar characteristics, namely, large differences in their dielectric constants and their performance as solvents. The new potential predicts a liquid/liquid phase separation, in good agreement with experimental data, and highlights the importance of the correct parametrization of the pure liquid phases to investigate liquid mixtures. Finally, we examine the microscopic origin of the observed immiscibility between formamide and hexan-2-one.

1. INTRODUCTION

Formamide is a highly polar molecule that forms strong hydrogen bonds through interactions between hydrogen and oxygen atoms lying in two different molecules ($\text{C}-\text{H}\cdots\text{O}$ and $\text{N}-\text{H}\cdots\text{O}$). The hydrogen bond character of the liquid makes formamide an excellent reference system to study the hydrophilic and hydrophobic interactions.¹ Further, formamide has attracted the attention of biologists and biochemists, since it is the smallest unit featuring in a peptidic chain. Also, formamide has been adopted as a model to investigate the formation and breaking of peptidic bonds.² The description of these bonds is essential to understand the physicochemical properties of proteins.

A considerable effort has been devoted in the past 30 years to develop force fields capable of accurately reproducing the

thermodynamic properties of complex fluids in a wide range of temperatures and pressures. Often, force fields have focused in reproducing the bulk density and heat of vaporization of liquids.^{3–5} This approach does not warranty the accurate prediction of all of the properties, and indeed deviations between simulation and experiment, e.g., critical temperature and orthobaric densities, have been reported.⁶ This has prompted the development of alternative parametrization strategies, targeting, e.g., the critical temperature and liquid coexistence density.^{7,8} However, very often these force fields fail to reproduce the dielectric constant of polar fluids.⁹ One possible reason for this may be connected to the approach used

Received: January 29, 2015



to derive the atomic charges, which has relied on quantum mechanical computations of molecules in vacuum, hence neglecting molecular correlations.

The properties of pure formamide have been investigated in a number of computer simulation studies.^{5,10} The latter approach takes into account multibody correlations but requires the use of a force field to compute the properties of the condensed phase. One of these force fields is the optimized potential for liquid simulations (OPLS), which was originally derived for amides by Jorgensen and Swenson in 1985.⁵ Later, in 1995, Essex and Jorgensen reported¹¹ the dielectric constant of formamide and dimethylformamide using isothermal isobaric Monte Carlo (MC) simulations with the OPLS force field.⁵ The simulation result for formamide, 59, is about half of the measured dielectric constant, 109. Pohuvski et al., in 2003,¹² reported the structural and dynamic properties of formamide using an intermolecular potential derived from *ab initio* computations. The force field was fitted to reproduce the structure obtained from neutron diffraction. Cordeiro¹³ in 1997 performed MC simulations to derive a force field of formamide able to reproduce the experimental liquid density and heat of vaporization. Bako et al. published later on¹⁴ an analysis of the hydrogen bond structure of formamide using the OPLS⁵ and Cordeiro's¹³ potentials. It has been suggested that the failure of current force fields to reproduce the dielectric constant of liquids is connected to the atomic charges that have been derived without considering intermolecular polarization effects, which would be relevant in condensed phases. One step in that direction is the computations of the dielectric properties of *N*-methylformamide and *N*-*N* methylformamide by Harder et al. in 2008, using polarizable force field based on the classical Drude oscillator.¹⁵ The simulation results were close to the experimental data. However, the improvement of polarizable force fields for the simulation of condensed phases might require the inclusion of higher dipole moments of the single molecules.

Recently, Coleman et al. reported¹⁶ an extensive investigation containing force field benchmark data for 146 organic liquids. The accuracy of the force fields OPLS/AA and GAFF (general Amber force field)^{3,4} to reproduce the liquid density, enthalpy of vaporization, heat capacity, surface tension, isothermal compressibility, volumetric thermal expansion coefficient, and dielectric constant was assessed. Most of the calculated properties agree well with the experimental results, but the surface tension and dielectric constant were systematically lower than the experiment. The deviations for surface tensions were ~70% and ~90% for GAFF and OPLS/AA, respectively. Zubillaga et al.¹⁷ revisited the OPLS/AA force field computations using a longer truncation distance for the Lennard-Jones dispersion interactions. The new surface tension results were in much better agreement with the experiment, highlighting the importance of long-range corrections in the computation of the pressure tensor. The dielectric constant calculated by Zubillaga et al.¹⁷ was not sensitive to changes on truncation distance. Both force fields, GAFF and OPLS/AA, underestimated the experimental dielectric constant of most of the 146 organic liquids by ~50%. For the specific case of formamide the dielectric constant at 298.15 K and 1 bar was 41 and 50 using GAFF and OPLS/AA force fields, respectively.

From the preceding discussion one may conclude that it is difficult to obtain the correct dielectric constant of formamide without including explicitly polarization effects. However, it has been shown recently^{9,18,19} that it is possible to reproduce the

experimental dielectric constant of water using nonpolarizable force fields. Alejandro et al. developed the TIP4Q and TIP4P/ ϵ nonpolarizable water force fields.^{18,19} The parameters were derived to reproduce simultaneously the liquid dielectric constant and the temperature of maximum density. Both models reproduced other thermodynamic and transport properties, including the water density anomalies. This work shows that rigid models can indeed reproduce the experimental data. We exploit this approach in this work.

In a recent work, Salas et al. introduced⁹ a procedure that enables the systematic derivation of a liquid force field, by fitting the atomic charges to reproduce the dielectric constant, and the Lennard-Jones (LJ) parameters, ϵ_{LJ} and σ_{LJ} , to reproduce the surface tension and liquid density, respectively. This procedure has been applied to methanol, pyridine, dichloromethane, and EMIM-BF₄ liquids. The resulting force fields represent an improvement over existing ones, providing generally a better representation of the experimental data. We note that the molecules investigated with that procedure do not have very high dipole moments. This enables the parametrization of charges and LJ parameters using a simple rescaling of the existing force fields parameters. We are interested in extending this methodology to derive force fields of highly polar molecules, such as formamide, and in particular reproduce the liquid dielectric constant. The latter property is an important input parameter in theories that model the solvent as a dielectric continuum, which have applications on solubility computations.

In this work we will test the applicability of the procedure introduced by Salas et al.⁹ to derive a new force field that describes the properties of liquid formamide. We will build on the work of Coleman et al.²⁰ and reparametrize the OPLS/AA force field. Advancing the discussion later we will show that rescaling the force field parameters is not enough to derive an accurate force field of formamide. This can be explained as a consequence of the strong hydrogen bonding between molecules, which depends very sensitively on the magnitude of the atomic charges. We present alternative strategies to fit the atomic charges, which rely on quantum mechanical computations and the introduction of polarization contributions, hence allowing us to successfully derive an accurate force field. Further, we test the transferability of our formamide force field to investigate liquid binary mixtures, in particular formamide/hexan-2-one. This binary mixture is a paradigm of a fluid consisting of two components with very different polar behavior.

The work is organized as follows. We first describe in section 2 the simulation details. An explanation of the different optimization procedures employed in this work follows. We then discuss our results and close the work with a summary of the main conclusions and final remarks.

2. FORCE FIELD AND SIMULATION DETAILS

We employ here a potential based on the OPLS/AA force field, which combines intramolecular terms (bond stretching and angle bending and torsion) with intermolecular and intramolecular nonbonded interactions.³ The OPLS/AA functional form for the intermolecular contributions contains Lennard-Jones and Coulombic terms,

$$V(r_{ij}) = \left\{ 4\epsilon_{ij} \left[\left(\frac{\sigma_{ij}}{r_{ij}} \right)^{12} - \left(\frac{\sigma_{ij}}{r_{ij}} \right)^6 \right] + \frac{q_i q_j}{4\pi\epsilon_0 r_{ij}} \right\} f_{ij} \quad (1)$$

where r_{ij} is the distance between atoms i and j , q_i is the partial charge on atom i , ϵ_0 is the vacuum permittivity, and σ_{ij} and ϵ_{ij} are the effective atom diameter and interaction strength, respectively. The factor $f_{ij} = 1.0$, except for intramolecular interactions between atom pairs separated by three bonds^{3,21} where the value is 0.5. The cross-interactions are calculated using the geometric mixing rules: $\sigma_{ij} = (\sigma_i \sigma_j)^{1/2}$ and $\epsilon_{ij} = (\epsilon_i \epsilon_j)^{1/2}$.

Molecular dynamics simulations in the isothermal–isobaric ensemble, *NPT*, with isotropic fluctuations of volume, were performed to compute the liquid density and dielectric constant at the standard pressure, 1 bar. These simulations involved typically 500 molecules. Simulations in the canonical ensemble, *NVT*, were also performed to compute the surface tension of the liquid, by simulating an explicit liquid–vapor interface containing, typically, 1000 molecules. The interface was generated by setting up a liquid slab surrounded by vacuum in a simulation box with periodic boundary conditions in the three spatial directions. The dimensions of the simulation cell were $L_x = L_y = 52 \text{ \AA}$ with $L_z = 3L_x$, with z being the normal direction to the liquid–vapor interface.

The GROMACS 4.5.4 package²² was employed in all of the simulations presented in this work. The equations of motion were solved using the leapfrog algorithm with a time step of 2 fs. The temperature was coupled to the Nosé–Hoover thermostat with a parameter $\tau_T = 0.2 \text{ ps}$ while the pressure was coupled to the Parrinello–Rahman barostat with a coupling parameter $\tau_p = 0.5 \text{ ps}$. The bond distances in the formamide molecule were kept rigid by using the LINCS algorithm,²³ and the molecule was maintained planar by using appropriate torsional angles. The electrostatic interactions were computed with the particle mesh Ewald approach²⁴ with a tolerance of 10^{-6} for the real space contribution, with a grid spacing of 1.2 \AA and spline interpolation of order 4. In the isotropic *NPT* simulations the real part of the Ewald summation and the LJ interactions were truncated at 12 \AA . Long range corrections for the LJ energy and pressure were included. The dielectric constant was computed by analyzing the dipole moment fluctuations of the simulation system.^{25,26}

The density and dielectric constant were calculated in the same simulation for at least 120 ns after an equilibration period of 10 ns. For the surface tension computations in the *NVT* ensemble the cutoff was set to 25 \AA , since the surface tension depends on the truncation of the interactions^{17,27} and the interface cross-sectional area.^{28,29} The equilibration period for the interfacial simulations was 2 ns, and the results for the average properties were obtained over an additional 6 ns trajectory. The equations used to calculate the dielectric constant, surface tension, self-diffusion coefficient, and pair distribution function are given as Supporting Information.

The quantum mechanical computations were performed with the Gaussian09 set of programs³⁰ using the M062X functional³¹ and the 6-311++g** basis set.^{32,33} The hybrid functional was chosen because it was parametrized with molecules containing nitrogen, and the basis set represents a good balance between computational cost and accuracy.

Among other approaches, we derived the atomic charges from populations analyses based on both charges from electrostatic potentials using a grid based method (CHELPG)³⁴

and Merz–Singh–Kollman (MK)^{35,36} schemes. The criteria for convergence of these approaches was based on energy, density, or orbital gradient.³⁷

3. RESULTS

First, *ab initio* calculations and molecular dynamics simulations were performed to obtain the optimum set of partial charges and the LJ parameters to determine dielectric constant, surface tension, and liquid density in good agreement with experimental data. At the end, the original and new force field of formamide were used to study a binary mixture between hexan-2-one and formamide to analyze their miscibility properties.

3.1. Rescaling the Atomic Charges. Rescaling of the atomic charges of weakly polar molecules⁹ has been successfully employed in the past. The method can be applied by perturbing the parameters of existing force fields and rescaling them to reproduce specific thermodynamic properties. We tested the accuracy of the OPLS/AA force field in determining the dielectric constant of formamide by performing *NPT* computer simulations at 298.15 K and 1 bar. In agreement with previous studies¹⁶ the dielectric constant, 50, is much lower than the experimental result, 109. Hence, as a first step to correct the force field we applied the method introduced by Salas et al.⁹ We rescaled linearly the charges only, while the rest of the force field parameters were the same as in the OPLS/AA force field. The liquid density, dielectric constant, and self-diffusion coefficient are reported in Table 1. The electrostatic

Table 1. Atomic Charges (Units of the Electron Charge) for the Original OPLS/AA Force Field^a

atom	$f_q = 1.0$	$f_q = 1.1$	$f_q = 1.2$	$f_q = 1.35$
C	0.500	0.550	0.600	0.675
O	−0.500	−0.550	−0.600	−0.675
HC	0.000	0.000	0.000	0.000
N	−0.760	−0.836	−0.912	−1.026
H	0.380	0.418	0.456	0.513
H	0.380	0.418	0.456	0.513
μ	4.20	4.62	5.04	5.68
ρ	1122.6	1152.2	1178.4	1202.1
ϵ	50.2	55.1	55.1	11.2
$\langle M \rangle$	1.32	2.23	6.07	110.82
$D/10^{-5}$	0.51	0.14	0.013	

^aThe charge scaling factor is f_q . The molecular dipole moment is μ (D). The liquid density is ρ (kg/m³), the average dipole moment of the system is $\langle M \rangle$ (D), and the self-diffusion coefficient is D (cm²/s). The experimental values are $\epsilon = 108.94$, $\rho = 1129.0 \text{ kg/m}^3$, and $D = 0.521 \times 10^{-5} \text{ cm}^2/\text{s}$.

interactions between the hydrogen bonding sites leads to an enhancement of the liquid structure, with formation of molecular clusters and a concomitant reduction of the liquid dynamics, which is reflected in a smaller diffusion coefficient at higher atomic charges (see Table 1).

3.2. Atomic Charges via *ab Initio* Computations. We have shown in the previous section that it is not possible to reproduce the experimental dielectric constant by simply rescaling the atomic charges of the OPLS/AA force field. We apply the following *ab initio* quantum chemical calculations in vacuum and also with polarization effects. We have considered approaches based on population analyses and fitting to the

molecular electrostatic potential (CHELPG and MK, and wave function analyses (Mulliken³⁸ and natural bond orbital (NBO)^{39,40}). We have collected all of our results for isolated molecules in vacuum in Table 2. These charges in combination

Table 2. Atomic Charges Derived from Different Population Analyses for Isolated Molecules in Vacuum: Mulliken, NBO, CHELPG, and MK^a

atom	Mulliken ³⁸	NBO ^{39,40}	CHELPG ³⁴	MK ^{35,36}
C	0.1203	0.5464	0.7267	0.6553
O	−0.3798	−0.6097	−0.5835	−0.5554
HC	0.1035	0.1045	0.0197	0.0128
N	−0.3919	−0.8346	−0.9407	−0.9623
H	0.2852	0.4000	0.4277	0.4423
H	0.2628	0.3934	0.3895	0.4073
μ	4.02	4.85	4.04	4.02
ρ	1094.7	1194.6	1146.8	1149.6
$\langle M \rangle$	1.5	10.5	0.8	2.2
ϵ	53.5	57.5	34.8	35.9
$D/10^{-5}$	1.20	0.04	0.28	0.30

^aThe variables μ , ρ , $\langle M \rangle$, ϵ , and D have the same meaning as units reported in Table 1. All data correspond to the thermodynamic state, 298.15 K and 1 bar. The experimental values are $\epsilon = 108.94$, $\rho = 1129.0 \text{ kg/m}^3$, and $D = 0.521 \times 10^{-5} \text{ cm}^2/\text{s}$.

with the rest of all original OPLS/AA parameters, including the bond distances and angles, were used to perform NPT molecular dynamics computations of the dielectric constant.

The values for the average dipole moment (see Table 2) indicate that our computations were well-converged. This can also be seen in the running average of the dielectric constant (see Figure 1), which reaches the average value in 20–40 ns. The results obtained with the different schemes and given in Table 2 are in poor agreement with experiment.

To check the effect of larger basis sets on the results, calculations using 6-311++g(2d,2p) and 6-311++g(df,pd) were performed within the MK approach. The molecular dipole moments were 4.04 and 4.06 D, respectively, compared with

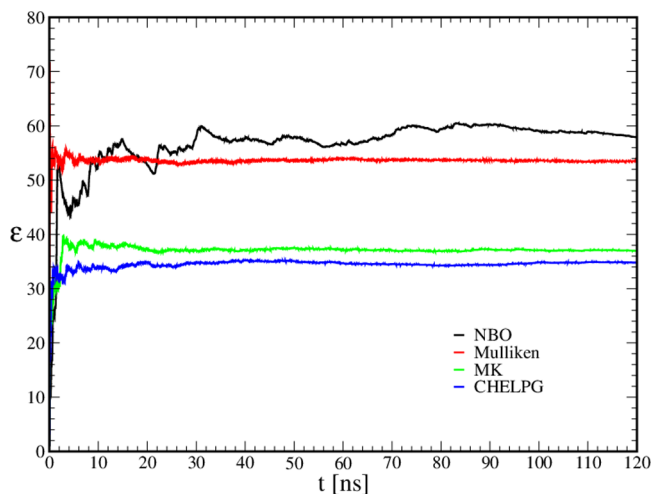


Figure 1. Results of the dielectric constant of formamide at 298.15 K and 1 bar using charges obtained from *ab initio* calculation on isolated molecules in vacuum using the Mulliken, NBO, MK, and CHELPG approaches. The rest of parameters were the original OPLS/AA values.

4.02 D obtained using a smaller basis set 6-311++g**. The poor performance of these charge distributions prompted us to consider polarization effects in our *ab initio* computations. These polarization effects are important in many chemical and biochemical processes in solution. Existing continuum models, e.g., the polarizable continuum model, takes into account the influence of the solvent through an effective dielectric constant.^{41–43} The solvation model density (SMD) by Marenich et al.⁴⁴ provides another alternative to handle these effects. The SMD approach was combined with the M062X functional and the same basis sets employed before (6-311++g**). The atomic charges were derived by using the population analysis methods mentioned earlier. We compile all of the results in Table 3. We found that the inclusion of the

Table 3. Atomic Charges Obtained from Different Population Analyses^a

atom	Mulliken	NBO	CHELPG	MK
C	0.1472	0.5562	0.7804	0.7079
O	−0.5561	−0.7537	−0.7709	−0.7450
HC	0.1845	0.1471	0.0178	0.0494
N	−0.4382	−0.8031	−0.9202	−0.9296
H	0.3341	0.4232	0.4614	0.4724
H	0.3285	0.4303	0.4315	0.4449
μ	5.71	6.33	5.80	5.83
ρ	1202.1	1334.2	1244.2	1283.3
$\langle M \rangle$	5.1	1718.0	1516.8	1821.2
ϵ	132.5			

^aThe polarization effects were taken into account through the SMD model.⁴⁴ The properties reported in the table have the same meaning and units as those in Tables 1 and 2. All of the simulations were performed in the NPT ensemble at 298.15 K and 1 bar.

polarization effects through the SMD method increases ~30% the molecular dipole moment, irrespective of the method employed for the population analysis. To obtain the dielectric constant and other properties, we performed NPT MD simulations of liquid formamide using the new charge distribution with all of the original OPLS/AA parameters, including bond distances and angles. The density increases slightly, ~10%, with respect to the data reported in Table 2, while the dielectric constant varies significantly depending on the method used to derive the atomic charges. The dielectric constant obtained from the Mulliken analysis, 132.5, was of the order of but higher than the experimental value, 109. We show in Figure 2A the final configuration, which clearly is a liquid-like phase. We found that the simulations with the other atomic charges (NBO, CHELPG, and MK) featured in general poor stability, with large fluctuations in the simulation cell dipole moment, which precluded the computation of reliable values for the dielectric constant. The highly negative and positive charges on the oxygen/nitrogen and carbon results in strong ordering. See Figure 2B–D. It is remarkable the strong impact that the atomic charges have in the formation of solid phases, with the molecules forming well-defined strings. Typical radial distribution functions are provided as Supporting Information.

3.3. Derivation of an Accurate Force Field for Liquid Formamide. We have shown that the direct application of standard *ab initio* approaches to fit the atomic charges does not provide an accurate force field to simulate the liquid phase of formamide. Hence, we considered the approach reported by

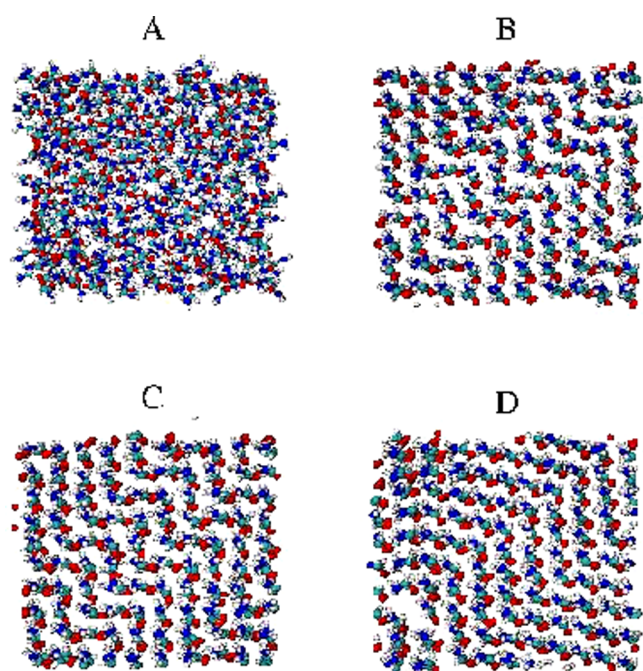


Figure 2. Typical snapshots of formamide systems simulated with charges derived from different approaches including polarizable effects: (A) Mulliken, (B) NBO, (C) CHELPG, and (D) MK.

Salas et al.⁹ First, we derived the atomic charges from the Mulliken analysis reported in the previous section in combination with the SMD approach. The charges were then optimized to match the experimental dielectric constant using molecular dynamics simulations, keeping constant the rest of the original OPLS/AA parameters. Then, we kept the optimal charges fixed and performed a rescaling of the OPLS/AA Lennard-Jones values for ϵ_{ij} to obtain the experimental surface tension. Finally, the original σ_{ij} OPLS/AA values were also linearly rescaled to obtain the experimental liquid density keeping constant the new charges and new ϵ_{ij} parameters. The details of the method are given in ref 9 and as Supporting Information.

The final optimized force field parameters are given in Table 4 and compared with those from the original OPLS/AA. We have collected in Table 5 the simulated and experimental data

Table 4. Original and New Parameters Obtained in This Work for the OPLS/AA Force Field

atom	q (e)	σ (nm)	ϵ (kJ/mol)
original			
C	0.5000	0.37500	0.43932
O	−0.5000	0.29600	0.87864
HC	0.0000	0.24200	0.06276
N	−0.7600	0.32500	0.71128
H	0.3800	0.00000	0.00000
H	0.3800	0.00000	0.00000
new			
C	0.1398	0.380625	0.307524
O	−0.5283	0.300440	0.615048
HC	0.1753	0.245630	0.043932
N	−0.4163	0.329875	0.497896
H	0.3174	0.000000	0.000000
H	0.3121	0.000000	0.000000

Table 5. Results at 298.15 K and 1 bar Using the OPLS/AA Force Field with the Original and New Parameters Obtained in This Work^a

Property	Original	New	Experiment ^{45,46}
ϵ	50.2	107.6	108.9
γ	61.3	57.2	57.0
ρ	1122	1128.5	1129.0

^aThe calculated relative errors respect to the experiment using the new parameters are 1.0%, 0.6%, and 0.04% for ϵ , γ , and ρ , respectively. The surface tension is given in mN/m and density in kg/m³.

at $T = 298$ K and $P = 1$ bar for the three target properties discussed earlier. The data show that the new force field provides a good description of the dielectric constant, surface tension, and liquid density. We have included in the Supporting Information the numerical data of the liquid density, dielectric constant, and surface tension for all of the systems investigated in this work.

An important element of a force field is the combination rules employed to compute the cross-interactions between atoms of different type. These rules define the transferability of the potential to simulate, e.g., mixtures. The OPLS/AA force field uses the geometric mixing rule, $\sigma_{ij} = (\sigma_{ii}\sigma_{jj})^{1/2}$, while other force fields, such as GAFF, use the so-called Lorentz–Berthelot where $\sigma_{ij} = (\sigma_{ii} + \sigma_{jj})/2$. The combination rule for ϵ_{ij} is the same in both force fields: $\epsilon_{ij} = (\epsilon_{ii}\epsilon_{jj})^{1/2}$. To test these different implementations of the combining rules, we run additional simulations to compute the target properties at 298.15 K. The liquid calculations were carried out at 1 bar. The factor f_{ij} appearing in eq 1 was identical in both mixing rules. The parameters obtained in this work are used in both calculations. The results are shown in Table 6. The combination rule is

Table 6. Results for the Target Properties Using the New Parameters but with Two Mixing Rules for σ_{ij} ^a

property	geometric	Lorentz–Berthelot	experiment
ϵ	107.6	105.7	108.9
γ	57.0	54.4	57.0
ρ	1128.5	1117.3	1129.0

^aThe surface tension is given in mN/m and the density in kg/m³.

shown to have a small impact on the liquid and interfacial properties, with a maximum deviation in the surface tension of $\sim 5\%$. The observed differences were within our target tolerance. Considering the small differences between both combination rules and because we want to compare results from the OPLS/AA force field, we will be using the geometric rule to perform the rest of the computations presented in this work.

In order to check the accuracy of our force field and the general improvement over the existing OPLS/AA potential, we performed additional *NPT* and *NVT* computations of liquid formamide as a function of temperature. The new force field parameters reproduce the experimental target properties within the requested tolerance in the available temperature range; see Figure 3. It has to be noted that formamide is not stable for temperatures above 373 K as it decomposes in hydrogen cyanide and water.⁴⁷ Overall, the new parametrization provides an improvement on all of the target properties over the existing OPLS/AA force field (Table 7). The relative error for the (original, new) parameters with respect experimental data are

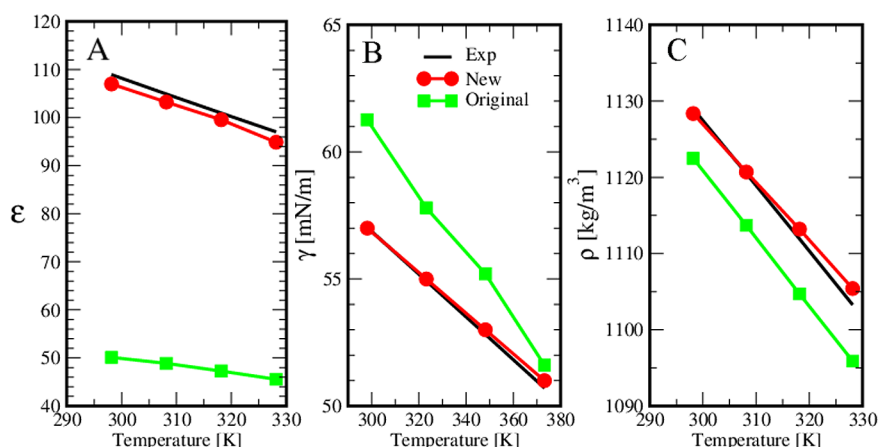


Figure 3. Results of target properties for formamide as a function of temperature using the OPLS/AA force field: (A) dielectric constant, (B) surface tension, and (C) liquid density. The results for the original and new parameters are shown with green squares and red circles, respectively. The experimental values are shown with continuous lines.

Table 7. Results of Dielectric Constant, Surface Tension (mN/m), and Liquid Density (kg/m³) of Formamide As a Function of Temperature (K) Obtained with the New Parameters for OPLS/AA

property	temperature	this work	experiment ^{45,46}
ϵ	298.15	107.6	108.94
	308.15	103.2	104.91
	318.15	99.6	100.94
	328.15	94.9	97.04
γ	298.15	57.7	57.0
	323.15	55.5	54.9
	348.15	53.5	52.8
	373.15	51.2	50.7
ρ	298.15	1128.5	1129.0
	308.15	1120.7	1120.5
	318.15	1113.3	1111.9
	328.15	1105.4	1103.3

(54%, 1%) for the dielectric constant, (7.0%, 0.6%) for the surface tension, and (0.6%, 0.04%) for the liquid density. We

have obtained a force field that reproduces the dielectric constant keeping the same time the accuracy in predicting density and surface tension.

3.4. Testing the Transferability of the New Force Field: The Hexan-2-one/Formamide Binary Mixture. In order to test the transferability of our new force field parameters, we studied a liquid binary mixture consisting of formamide and hexan-2-one. As noted in the Introduction, this mixture is a stringent test as it involves two polar liquids with significantly different dielectric constants. Further, hexan-2-one is a ketone used in industrial applications as a general solvent and in paints. It has a low dielectric constant (15) at 298.15 K and liquid density of 807 kg/m³.¹⁶ It is known that this molecule has low solubility in water, 14 g/L,⁴⁸ while formamide shows a much higher solubility in water, 1000 g/L.⁴⁷ Due to a lack of experimental data, we mixed both components at $T = 293$ K in our laboratory and found that they formed a well-defined liquid/liquid phase equilibrium. We did not attempt to measure densities or composition of the liquid mixtures; work

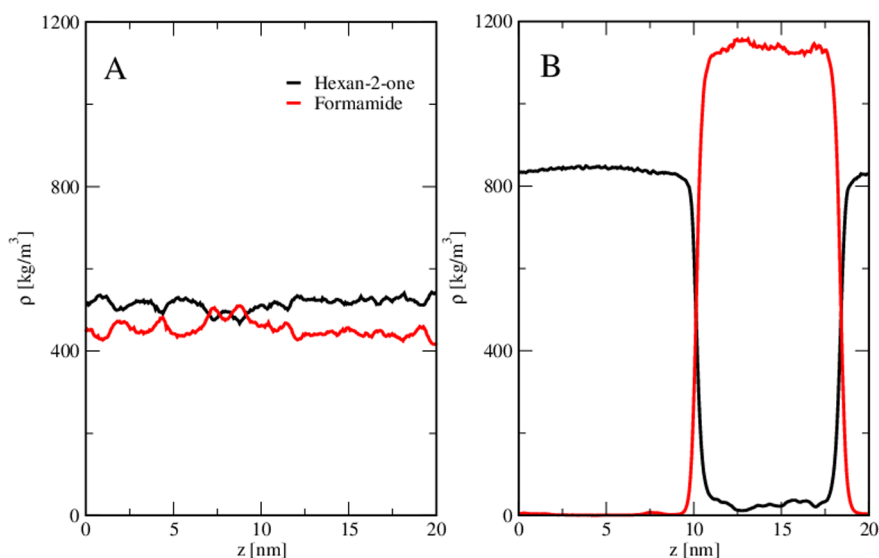


Figure 4. Density profiles of the hexan-2-one/formamide mixture: (A) original OPLS/AA parameters for both components. (B) original OPLS/AA for hexa-2-one and the new parameters derived in this work for formamide.

in that direction is being performed. A picture of our experiment is included in the Supporting Information.

First, a liquid simulation with 256 hexan-2-one molecules was performed at 298.15 K and 1 bar, with the original OPLS/AA force field parameters, obtaining a liquid density of 821 kg/m³ and dielectric constant of 10.5 in acceptable agreement with experimental and simulation data.¹⁶

To analyze and compare the accuracy of the original OPLS/AA and new parameters derived here for formamide, we performed NVT simulations of the mixture at 298.15 K. Two pre-equilibrated configurations of formamide and hexan-2-one were placed side by side in an elongated simulation cell such that the two liquids were initially completely demixed. In one simulation we employed the original OPLS/AA parameters for both components, while in a second independent run we used the original parameters for hexan-2-one and the new OPLS/AA parameters for formamide. The cross-interactions were computed with the geometric combining rules. Long simulations involving 250 ns of equilibration and up to 2.3 μ s of production time were performed to ensure a proper relaxation of the system. We computed the density profile of every component for different subaverages to follow the miscibility. The results for the first simulation averaged over the last 25 ns are shown in Figure 4A. We find that the original OPLS/AA predicts complete miscibility between both liquids. For the second simulation, which was performed with the new formamide potential derived in this work we find that the two liquids form a well-defined liquid–liquid interface (see Figure 4B), hence clearly showing that they are immiscible, a result that is expected in view of the large difference in dielectric constant. The latter result is consistent with our experiment.

In order to understand the role of molecular interactions in the solubility of the mixtures studied previously, the free energy of solvation of a hexan-2-one molecule in a liquid formamide was obtained using the thermodynamic integration, TI, method.^{49–51} Details and results of the TI are presented in the Supporting Information.

The free energy to add a hexan-2-one molecule from formamide, both with the original OPLS/AA parameters, was of $\Delta G = -22.84$ kJ/mol while its value with the new formamide parameters was $\Delta G = -15.96$ kJ/mol. Clearly the new charge distribution makes less favorable the solution of hexan-2-one in formamide. This is consistent with our experiment. The free energy provides insights about the importance of the charge distribution in describing the miscibility.

4. CONCLUSIONS

We have presented a systematic procedure that combines *ab initio* and molecular dynamics computations, which allows the derivation of optimum parameters for the formamide force field. The approach targets three different properties: the dielectric constant, liquid density, and surface tension. These properties are fitted by systematically rescaling, the atomic charges, and the interaction strength (ϵ_{LJ}) and atomic diameters (σ_{LJ}) appearing in the Lennard-Jones potential used to describe the dispersion interactions. First the charges from the new *ab initio* calculations with polarizable effects using the Mulliken approach were rescaled to reproduce the dielectric constant. Second, the Lennard-Jones parameters ϵ_{LJ} were fitted to match the surface tension at the vapor–liquid interface, and finally in a third step the σ_{LJ} parameters were fitted to reproduce the liquid density. Two cycles were needed to find the optimum parameters. The idea behind the method is that a

change in a specific force field parameter affects more one property than the others. The parameters can then be fitted independently if appropriate target properties are chosen. For instance, changes in the ϵ_{LJ} affect much more the surface tension than dielectric constant and liquid density. Starting from the widely used OPLS/AA force field we derived new parameters that provide a good prediction of the liquid density, surface tension, and crucially the dielectric constant of liquid formamide. The new model represents a significant improvement in the prediction of this quantity, which is now in very good agreement with the experiment. The previous OPLS/AA parameters underestimated this property by over 50%. Although the parameters were fitted at 298.15 K, they show good transferability in the prediction of the liquid properties at higher temperatures. We did also analyze the impact of the combination rules in the accuracy of the force field. We find that the results are fairly independent of whether the geometric or Lorentz–Berthelot combination rules are employed to derive cross-interactions between dissimilar atoms.

We performed additional simulations of a liquid–liquid mixture, consisting of hexan-2-one and formamide. This mixture provides a further benchmark to test the transferability of our force field parameters. We have shown that the miscibility behavior is strongly dependent on the force field used. The original OPLS/AA parameters predict full miscibility, while the new force field for formamide predicts that the two liquids are immiscible, in good agreement with experiments performed in our laboratory.

The results from this work also show that polarizable models are not needed to obtain the dielectric constant and surface tension of highly polar fluids and to describe the miscibility of mixtures.

■ ASSOCIATED CONTENT

Supporting Information

Definitions and numerical results of thermodynamic, structural, and electric properties, selected pair distributions for the systems studied in this work, and the free energy change as a function of λ . This material is available free of charge via the Internet at <http://pubs.acs.org>.

■ AUTHOR INFORMATION

Corresponding Author

*E-mail: jra@xanum.uam.mx.

Funding

A.P.L. and E.N.-R. thank Conacyt for a Ph.D. and postdoctoral scholarship, respectively. F.B. thanks the EPSRC (Grant EP/J003859/1) and The Research Council of Norway (Project 221675) for financial support.

Notes

The authors declare no competing financial interest.

■ ACKNOWLEDGMENTS

G.A.M.-M., E.N.-R., and J.A. thank Laboratorio de Super-cómputo for allocation time. The authors would like to thank Ana María Soto Estrada for helping us with the Hexa-2-one/Formamide experiment.

■ REFERENCES

- (1) Puhovski, U. P.; Rode, B. M. Structure and dynamics of liquid formamide. *Chem. Phys.* **1995**, *190*, 61–82.

- (2) Kritsana, P.; Reinhart, A. A test particle model potential for formamide and molecular dynamics simulations of the liquid. *J. Chem. Phys.* **1987**, *86*, 5117–5145.
- (3) Jorgensen, W. L.; Maxwell, D. S.; Tirado-Rives, J. Development and All-Atom Force Field on Conformational Energetics and Properties of Organic Liquid. *J. Am. Chem. Soc.* **1996**, *118*, 11225–11236.
- (4) Wang, J.; Wolf, R. M.; Caldwell, J. W.; Kollman, P. A.; Case, D. A. Development and Testing of a General Amber Force Field. *J. Comput. Chem.* **2004**, *25*, 1157–1174.
- (5) Jorgensen, W. L.; Swenson, C. J. Optimized Intermolecular Potential Functions for Amides and Peptides. Structure and Properties of Liquid Amides. *J. Am. Chem. Soc.* **1985**, *107*, 569–578.
- (6) van Leeuwen, M. E.; Smit, B. J. Molecular Simulation of the Vapor–Liquid Coexistence Curve of Methanol. *J. Phys. Chem.* **1995**, *99*, 1831–1833.
- (7) Wick, C. D.; Stubbs, J. M.; Rai, N.; Siepmann, J. I. Transferable Potentials for Phase Equilibria. 7. Primary, Secondary, and Tertiary Amines, Nitroalkanes and Nitrobenzene, Nitriles, Amides, Pyridine, and Pyrimidine. *J. Phys. Chem. B* **2005**, *109*, 18974–18982.
- (8) Nath, S. K.; Escobedo, F. A.; de Pablo, J. On the simulation of vapor-liquid equilibria for alkanes. *J. Chem. Phys.* **1998**, *108*, 9905–9911.
- (9) Salas, F. J.; Méndez-Maldonado, G. A.; Núñez-Rojas, E.; Aguilar-Pineda, G. E.; Domínguez, H.; Alejandre, J. *J. Chem. Theory Comput.* **2015**, *11*, 683–693.
- (10) Xie, W.; Pu, J.; Mackerell, A. D.; Gao, J. Development of a Polarizable Intermolecular Potential Function (PIPF) for Liquid Amides and Alkanes. *J. Chem. Theory Comput.* **2007**, *3*, 1878–1889.
- (11) Essex, J. W.; Jorgensen, W. L. Dielectric constants of formamide and dimethylformamide via computer simulation. *J. Phys. Chem.* **1995**, *99*, 17956–17962.
- (12) Puhovski, Y. P.; Safonova, L. P.; Rode, B. M. Molecular dynamic simulations of a liquid formamide and N,N-dimethylformamide with new quantum mechanical potential. *J. Mol. Liq.* **2003**, *103–104*, 15–31.
- (13) Cordeiro, J. M. M. C. (Single Bond)H(Dotted Bond)O and N(Single Bond)H(Dotted Bond)O hydrogen bonds in liquid amides investigated by Monte Carlo simulation. *Int. J. Quantum Chem.* **1997**, *65*, 709–717.
- (14) Bako, I.; Megyes, T.; Bálint, S.; Chihaia, V.; Bellissent-Funel, M. C.; Krienke, H.; Kopf, A.; Suh, S. H. Hydrogen bonded network properties in liquid formamide. *J. Chem. Phys.* **2010**, *132*, No. 014506.
- (15) Harder, E.; Anisimov, V. M.; Whitfield, T.; MacKerell, A. D., Jr.; Roux, B. Understanding the Dielectric Properties of Liquid Amides from a Polarizable Force Field. *J. Phys. Chem. B* **2008**, *112*, 3509–3521.
- (16) Coleman, C.; van Maaren, P. J.; Hong, M.; Hub, J. S.; Costa, L. T.; van der Spoel, D. Force Field Benchmark of Organic Liquids: Density, Enthalpy of Vaporization, Heat Capacities, Surface Tension, Isothermal Compressibility, Volumetric Expansion Coefficient, and Dielectric Constant. *J. Chem. Theory Comput.* **2012**, *8*, 61–74.
- (17) Zubillaga, R. A.; Labastida, A.; Cruz, B.; Martínez, J. C.; Sánchez, E.; Alejandre, J. Surface Tension of Organic Liquids Using the OPLS/AA Force Field. *J. Chem. Theory Comput.* **2013**, *9*, 1611–1615.
- (18) Alejandre, J.; Chapela, G. A.; Saint-Martin, H.; Mendoza, N. A non-polarizable model of water that yields the dielectric constant and the density anomalies of the liquid: TIP4Q. *Phys. Chem. Chem. Phys.* **2011**, *13*, 19728–19740.
- (19) Fuentes-Azcatl, R.; Alejandre, J. Non-Polarizable Force Field of Water Based on the Dielectric Constant: TIP4P/e. *J. Phys. Chem. B* **2014**, *118*, 1263–1272.
- (20) <http://www.virtualchemistry.org>.
- (21) Jorgensen, W. L.; Tirado-Rives, J. The OPLS [optimized potentials for liquid simulations] potential functions for proteins, energy minimizations for crystals of cyclic peptides and crambin. *J. Am. Chem. Soc.* **1988**, *110*, 1657–1666.
- (22) Hess, B.; Kutzner, C.; van der Spoel, D.; Lindahl, E. GROMACS 4: Algorithms for highly efficient, load-balanced, and scalable molecular simulation. *J. Chem. Theory Comput.* **2008**, *4*, 435–447.
- (23) Hess, B.; Bekker, H.; Berendsen, H. J. C.; Fraaije, J. G. E. M. LINCS: A linear constraint solver for molecular simulations. *J. Comput. Chem.* **1997**, *18*, 1463–1472.
- (24) Essmann, U.; Perera, L.; Berkowitz, M. L.; Darden, T.; Lee, H.; Pedersen, L. G. A smooth particle mesh Ewald method. *J. Chem. Phys.* **1995**, *103*, 8577–8592.
- (25) Hansen, J. P.; McDonald, I. R. *Theory of Simple Liquids*, 4th ed.; Elsevier: Amsterdam, 2013.
- (26) Neumann, M. Dipole moment fluctuation formulas in computer simulations of polar systems. *Mol. Phys.* **1983**, *50*, 841–845.
- (27) Truckymchuk, A.; Alejandre, J. Computer simulations of liquid/vapor interface in Lennard-Jones fluids: Some questions and answers. *J. Chem. Phys.* **1999**, *111*, 8510–8523.
- (28) Orea, P.; López-Lemus, J.; Alejandre, J. Oscillatory surface tension due to finite-size effects. *J. Chem. Phys.* **2005**, *123*, 114702–114813.
- (29) Gonzalez-Melchor, M.; Bresme, F.; Alejandre, J. Molecular dynamics simulations of the surface tension of ionic liquids. *J. Chem. Phys.* **2005**, *122*, 104710-1–104710-8.
- (30) Frisch, M. J.; Trucks, G. W.; Schlegel, H. B.; Scuseria, G. E.; Robb, M. A.; Cheeseman, J. R.; Scalmani, G.; Barone, V.; Mennucci, B.; Petersson, G. A.; Nakatsuji, H.; Caricato, M.; Li, X.; Hratchian, H. P.; Izmaylov, A. F.; Bloino, J.; Zheng, G.; Sonnenberg, J. L.; Hada, M.; Ehara, M.; Toyota, K.; Fukuda, R.; Hasegawa, J.; Ishida, M.; Nakajima, T.; Honda, Y.; Kitao, O.; Nakai, H.; Vreven, T.; Montgomery, J. A., Jr.; Peralta, J. E.; Ogliaro, F.; Bearpark, M.; Heyd, J. J.; Brothers, E.; Kudin, K. N.; Staroverov, V. N.; Keith, T.; Kobayashi, R.; Normand, J.; Raghavachari, K.; Rendell, A.; Burant, J. C.; Iyengar, S. S.; Tomasi, J.; Cossi, M.; Rega, N.; Millam, J. M.; Klene, M.; Knox, J. E.; Cross, J. B.; Bakken, V.; Adamo, C.; Jaramillo, J.; Gomperts, R.; Stratmann, R. E.; Yazyev, O.; Austin, A. J.; Cammi, R.; Pomelli, C.; Ochterski, J. W.; Martin, R. L.; Morokuma, K.; Zakrzewski, V. G.; Voth, G. A.; Salvador, P.; Dannenberg, J. J.; Dapprich, S.; Daniels, A. D.; Farkas, O.; Foresman, J. B.; Ortiz, J. V.; Cioslowski, J.; Fox, D. J. *Gaussian 09*, Revision B.01; Gaussian: Wallingford, CT, USA, 2010.
- (31) Zhao, Y.; Truhlar, D. G. The M06 suite of density functionals for main group thermochemistry, thermochemical kinetics, non-covalent interactions, excited states, and transition elements: Two new functionals and systematic testing of four M06-class functionals and 12 other functionals. *Theor. Chem. Acc.* **2008**, *120*, 215–241.
- (32) McLean, A. D.; Chandler, G. S. Contracted Gaussian-basis sets for molecular calculations. 1. 2nd row atoms, Z=11–18. *J. Chem. Phys.* **1980**, *72*, 5639–5648.
- (33) Raghavachari, K.; Binkley, J. S.; Seeger, R.; Pople, J. A. Self-Consistent Molecular Orbital Methods. 20. Basis Set for Correlated Wave-Functions. *J. Chem. Phys.* **1980**, *72*, 650–654.
- (34) Breneman, C. M.; Wiberg, K. B. Determining atom-centered monopoles from molecular electrostatic potentials. The need for high sampling density in formamide conformational analysis. *J. Comput. Chem.* **1990**, *11*, 361–373.
- (35) Singh, U. C.; Kollman, P. A. An approach to computing electrostatic charges for molecules. *J. Comput. Chem.* **1984**, *5*, 129–145.
- (36) Besler, B. H.; Merz, K. M., Jr.; Kollman, P. A. Atomic charges derived from semiempirical methods. *J. Comput. Chem.* **1990**, *11*, 431–439.
- (37) Schlegel, H. B.; McDouall, J. J. In *Computational Advances in Organic Chemistry*; Ögretir, C., Csizmadia, I. G., Eds.; Kluwer Academic: Dordrecht, The Netherlands, 1991; pp 167–185.
- (38) Mulliken, R. S. Electronic Population Analysis on LCAO-MO Molecular Wave Functions. *J. Chem. Phys.* **1955**, *23*, 1833–1840.
- (39) Foster, J. P.; Weinhold, F. Natural hybrid orbitals. *J. Am. Chem. Soc.* **1980**, *102*, 7211–7218.
- (40) Reed, A. E.; Weinhold, F. Natural bond orbital analysis of near-Hartree–Fock water dimer. *J. Chem. Phys.* **1983**, *78*, 4066–4073.

- (41) Miertuš, S.; Scrocco, E.; Tomasi, J. Electrostatic interaction of a solute with a continuum. A direct utilization of *ab initio* molecular potentials for the prevision of solvent effects. *Chem. Phys.* **1981**, *55*, 117–129.
- (42) Miertuš, S.; Tomasi, J. Approximate evaluations of the electrostatic free energy and internal energy changes in solution processes. *Chem. Phys.* **1982**, *65*, 239–245.
- (43) Pascual-Ahuir, J. L.; Silla, E.; Tuñón, I. GEPOL: An improved description of molecular surfaces. III. A new algorithm for the computation of a solvent-excluding surface. *J. Comput. Chem.* **1994**, *15*, 1127–1138.
- (44) Marenich, A. V.; Cramer, C. J.; Truhlar, D. G. Universal Solvation Model Based on Solute Electron Density and on a Continuum Model of the Solvent Defined by the Bulk Dielectric Constant and Atomic Surface Tensions. *J. Phys. Chem. B* **2009**, *113*, 6378–6396.
- (45) Lide, D. R. *CRC Handbook of Chemistry and Physics*, 90 th ed.; CRC Press: Cleveland, OH, USA, 2009.
- (46) Yaws, C. L. *Thermophysical properties of chemicals and hydrocarbons*; William Andrew: New York, NY, USA, 2088 (April).
- (47) *Kirk-Othmer Encyclopedia of Chemical Technology*, 3 rd ed.; John Wiley and Sons: New York, NY, USA, 1980.
- (48) Flick, E. W. *Industrial Solvents Handbook*, 3 rd ed.; Noyes: Park Ridge, NJ, USA, 1985.
- (49) Villa, A.; Mark, A. E. Calculation of the Free Energy of Solvation for Neutral Analogs of Amino Acids Side Chains. *J. Comput. Chem.* **2002**, *23*, 548–553.
- (50) Pohorille, A.; Jarzynski, C.; Chipot, C. Good Practices in Free-Energy Calculations. *J. Phys. Chem. B* **2010**, *114*, 10235–10253.
- (51) Christ, C. D.; Mark, A. E.; van Gunsteren, W. F. Basic Ingredients of Free Energy Calculations: A Review. *J. Comput. Chem.* **2009**, *31*, 1569–1582.